CHAPTER 4

Paroxysmal non-kinesigenic dyskinesia is caused by mutations of the MR-1 mitochondrial targeting sequenze

Daniele Ghezzi[1], Carlo Viscomi[1], Alessandra Ferlini[2], Francesca Gualandi[2], Paolo Mereghetti[3], Domenico DeGrandis[4] and Massimo Zeviani[1,*]

[1] Unit of Molecular Neurogenetics—Pierfranco and Luisa Mariani Center for the Study of Children's Mitochondrial Disorders, National Neurological Institute 'Carlo Besta', Milan, Italy [2] Department of Experimental Medicine and Diagnostics, University of Ferrara, Ferrara, Italy [3] Department of Biotechnology and Biosciences, University of Milan-Bicocca, Milan, Italy [4] Division of Neurosciences, Public Health Hospital, Rovigo, Italy

ABSTRACT

Paroxysmal non-kinesigenic dyskinesia (PNKD) is an autosomal-dominant movement disorder characterized by attacks of dystonia, chorea and athetosis. Myofibrillogenesis regulator-1 (*MR-1*), the gene responsible for PNKD, is transcribed into three alternatively spliced forms: long (MR-1L), medium (MR-1M) and small (MR-1S). Two mutations, A7V and A9V, were previously discovered in the N-terminal region common to MR-1L and MR-1S. We now found a third mutation, A33P, in a new PNKD patient in the same region. Contrary to previous reports, we show here that the mutation-free MR-1M is localized in the Golgi apparatus, ER and plasma membrane, whereas both MR-1L and MR-1S isoforms are mitochondrial proteins, imported into the organelle thanks to a 39 amino acid-long, N-terminal mitochondrial targeting sequence (MTS). The MTS, which contains all three PNKD mutations, is then cleaved off the mature proteins before their insertion in the inner mitochondrial membrane. Therefore, mature MR-1S and MR-1L of PNKD patients are identical to those of normal subjects. We found no difference in import efficiency and protein maturation between wild-type and mutant MR-1 variants. These results indicate that PNKD is due to a novel disease mechanism based on a deleterious action of the MTS.

INTRODUCTION

Myofibrillogenesis regulator-1 (*MR-1*) (OMIM*609023) is a gene first identified from a skeletal muscle cDNA library, located on human chromosome 2q35 (1). Alternatively spliced variants give rise to three isoforms (Fig.1A): long (MR-1L, 385 amino acids), medium (MR-1M,

361 amino acids) and short (MR-1S, 142 amino acids). MR-1S and MR-1L share the first 79 N-terminal amino acids including the three PNKD mutations, whereas the MR1-M N-terminus consists of a different sequence composed of 55 amino acids. The MR-1L and MR-1M C-terminal sequence is identical and contains a β-lactamase domain similar to that of glyoxylase II, Glyo II. MR-1S and MR-1M are ubiquitously expressed, whereas MR-1L is present only in the brain (2,3). This gene is responsible for autosomal-dominant paroxysmal non-kinesigenic dyskinesia (PNKD, OMIM #118800) (2,3). PNKD consists of attacks of dystonia, chorea and athetosis, lasting from minutes to hours, which may occur either spontaneously at rest or following provoking factors, such as alcohol or caffeine assumption, emotional stress and fatigue. The onset is in childhood or early adulthood. Benzodiazepines (clonazepam) and a sodium-channel blocker (mexiletine), used as a myorelaxant, are the most effective medications.

Only two MR-1 mutations (A7V and A9V) have been reported to segregate with the disease in 14 unrelated PNKD families of European ancestry and in one family from Oman (2–6). Haplotype analysis excluded the presence of a recent common ancestor among some of these families, suggesting independent mutational events (4). Both the A7V and A9V changes are in the N-terminal region common to isoforms MR-1L and MR-1S, but not MR-1M, and occur in a predicted amino-terminal α-helix (Fig.1B). The MR1-M isoform, which is not mutated in PNKD, was previously reported to localize to mitochondria, whereas the MR-1S and MR-1L isoforms, which both

carry the PNKD mutations, were attributed to the cytosolic or plasma membrane compartments.
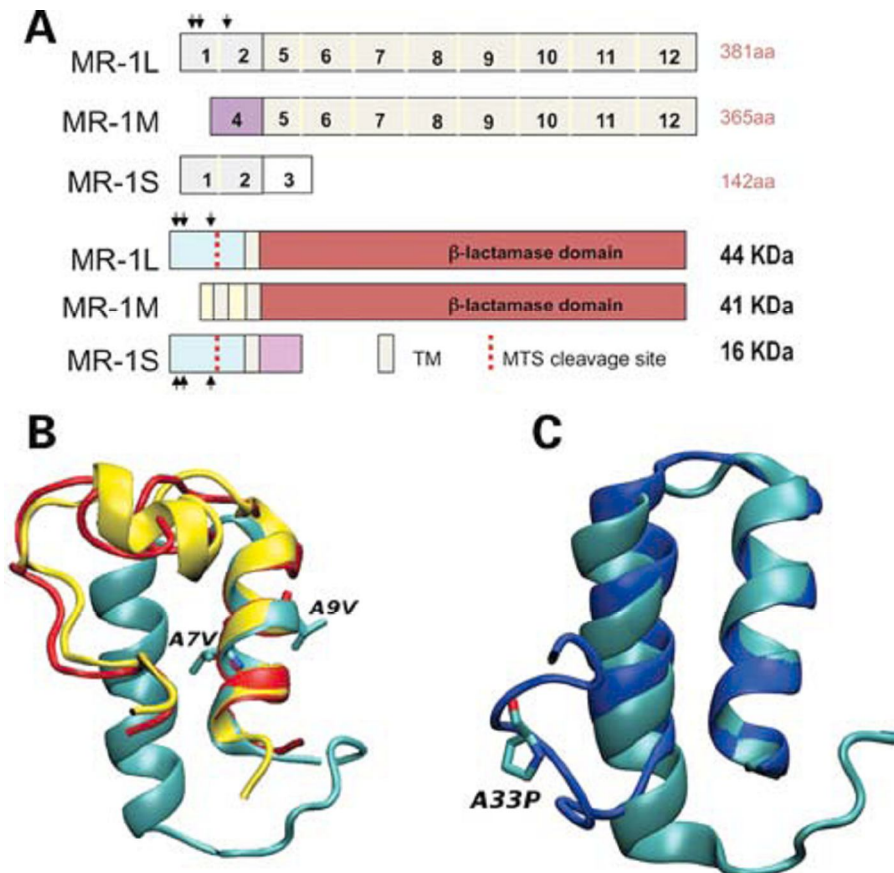
Figure1. (**A**) Schematic structure of the three MR-1 cDNAs (top) and protein isoforms (bottom). Coding exons are numbered; arrows indicate the position of A7V, A9V and A33P mutations; dot lines show the predicted MTS cleavage site, between amino acids 39 and 40. (**B**) Superposition of MR1-WT model (cyan) with the MR1-A7V model (yellow) and MR1-A9V model (red). Notice that the A7V and A9V changes disrupt the second α-helix. (**C**) Superposition of MR1-WT model (cyan) with the MR1-A33P model (blue). Notice that the A33P is associated with a structurally aberrant C-terminus.

As a result, PNKD was concluded not to be a mitochondrial-related disorder. However, the MR-1S and MR-1L N-terminal sequence scores consistently high when analyzed by biocomputational prediction software for mitochondrial targeting, whereas the

intermediate MR-1M isoform gives controversial results (Table1). This observation prompted us to re-characterize experimentally the localization, post-translational processing and biochemical features of the MR-1 isoforms using a recombinant cell culture system. In addition, we found a further PNKD patient with a novel mutation, again localized in the N-terminus of MR-1L and MR-1S isoforms (Fig.1C).

Table1. Prediction of mitochondrial localization for MR-1 isoforms

	MitoProt (%)	TargetP (%)	Predotar (%)	WoLF-PSORT
MR-1L	99	99	67	23/32
MR-1M	98	3	1	0/32
MR-1S	92	84	69	16/32

PATIENT

Since early childhood, this 57-year-old obese man experienced recurrent episodes of involuntary movements, lasting several minutes and consisting of a sense of muscle tightening, followed by dystonic posturing of the extremities. Choreoathetotic movements of tongue and neck start as an unpleasant sensation, prompting him to protrude his tongue out of his mouth. Blepharospasm can accompany the paroxysmal episodes. The involuntary movements are triggered by fatigue, emotional stress or exposure to bright light. He also suffers from recurrent attacks of cerebellar ataxia with unsteady gait and slurred speech. In addition, he reports difficulty in opening his mouth when exposed to a cold environment, and stiffness or blockage of his arm when touching a cold object. Neurological examination between crises was consistently normal. Routine blood tests showed no significant alterations. Mexiletine 500 mg/day produced partial

improvement with reduction of the sense of tightening. His father, a paternal half-brother and his grandfather (Fig.2A) presented episodes of blepharospasm and severe muscle cramps with difficulty in stair climbing, indicating dominant transmission of the trait. These family members were unavailable for further studies.
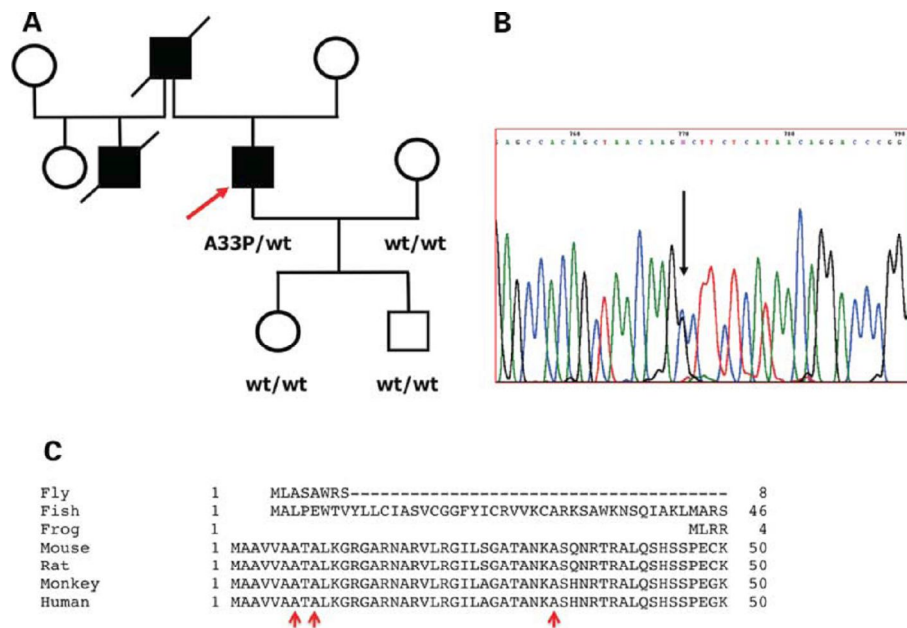

Figure2. (**A**) Pedigree of the PNKD patients. Filled symbols indicate affected individuals. (**B**) Sequence analysis of exon 2 of MR-1 showing the heterozygous c.G97C mutations in the PNKD patient. (**C**) Clustal-W alignment of the MR-1 N-terminus in different animals. Notice that the sequence is conserved in mammals but not in non-mammalian species. Red arrows indicate the PNKD mutant amino acid residues.

RESULTS

By analyzing the entire coding sequence of the *MR-1* gene (1,2), we identified a heterozygous c.97G>C transversion in the MR-1L and MR-1S cDNAs, predicting a p.A33P amino acid change in the N-terminus (Fig.2B). A total of 500 control chromosomes resulted negative for the c.97G>C variation. The MR-1L and MR-1S N-

terminus is highly conserved in mammals, including positions A7, A9 and A33 (Fig.2C), but not in other eukaryotes.
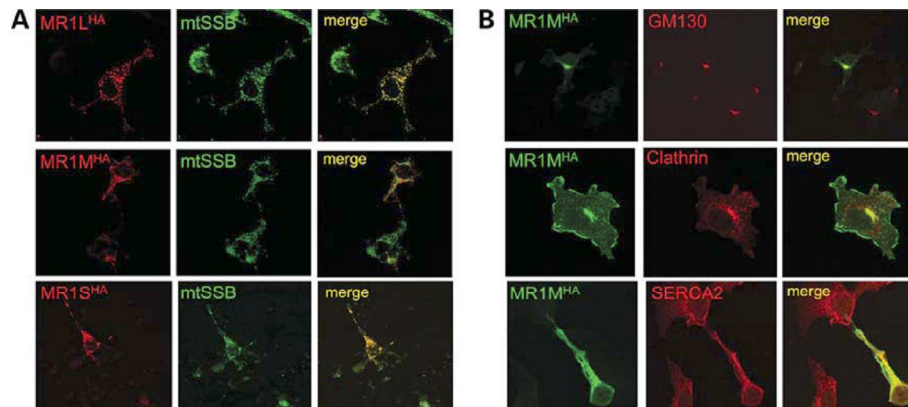
Figure3. Confocal IF images of COS7 cells transfected with MR-1L^{HA}, MR-1M^{HA} and MR-1S^{HA}. (**A**) The IF pattern obtained using an anti-HA-specific monoclonal antibody is in red. In green are the IF patterns obtained using a polyclonal antibody against the mtSSB protein (7). (**B**) The IF pattern obtained using an anti-HA-specific polyclonal antibody is in green. In red are the IF patterns obtained using commercially available monoclonal antibodies against the Golgi matrix protein 130 kDa, GM130; Clathrin (localized to Golgi and vesicles); sarcoplasmic reticulum/ER calcium ATPase 2, SERCA2.

In order to establish the subcellular localization of the MR-1 isoforms, confocal immunofluorescence (IF) microscopy was performed on COS7 and HeLa cells transiently or stably expressing recombinant MR-1 variants, which carried a 9 amino acid-long hemoagglutinin (HA) tag at the C-terminus (7). Both MR-1L^{HA} and MR-1S^{HA} IF patterns were coincidental to that of the single-stranded mtDNA protein (mtSSB) (Fig.3A). In contrast, the HA-specific immunolocalization in COS7^{MR-1M} (Fig.3B) and HeLa^{MR-1M} (Supplementary Material, Fig. S1) cells was >90% in the Golgi, the rest being in the endoplasmic reticulum (ER) and plasma membrane.

Notably, no MR-1M-specific IF signal was detected in mitochondria and peroxisomes (Fig.3A).

These data were confirmed by western blot (WB) analysis on subcellular fractions (Fig.4A). Each MR-1^{HA} species was detected in the 13 000g fraction (P13) containing mitochondria, peroxisomes and the Golgi (8). However, HA-specific cross-reacting material (CRM) was present also in the 100 000g fraction (P100) of the HeLa^{MR-1M} cell line, corresponding to microsomes and plasma membrane fragments, whereas no HA-CRM was detected in the same fraction of HeLa^{MR-1L} and HeLa^{MR-1S} cell lines. WB analysis on suborganellar fractions showed that MR-1S was present only in the mitochondrial membrane fraction, whereas MR-1L was mainly in the membrane fraction but was also present in the soluble fraction (Fig.4A).

To demonstrate active mitochondrial import, each radiolabeled *in vitro*-translated MR-1^{HA} isoform was incubated in different conditions with freshly prepared, energized mitochondria (8). This analysis demonstrated that MR-1L and MR-1S, but not MR-1M, are imported into mitochondria through the $\Delta\Psi$-dependent TOM–TIM import machinery (9,10), which targets proteins to the inner mitochondrial compartment. After translocation, the MTS is cleaved off the MR-1L and MR1-S mature protein species by the mitochondrial processing peptidase (11) (Fig.4B). These data are in agreement with biocomputational analysis, which predicts for both protein species the presence of a single transmembrane domain, stronger for MR-1S than for MR-1L (Supplementary Material, Table S1). The mature forms of MR-1L^{HA} and MR-1S^{HA} from recombinant HeLa cell lines were clearly smaller than the corresponding *in vitro*-translated products

encompassing their entire open-reading frames (ORFs), although no difference was detected for MR-1M (Fig.4C). These results further indicate that, in contrast with MR-1M, the MR-1L and MR-1S precursor proteins undergo a post-translational processing consisting in the elimination of the MTS.

To further define the topological position within the inner mitochondrial membrane (IMM), we treated with proteinase K (PK) both intact mitochondria and mitoplasts (12), i.e. organelles deprived of the outer membrane, isolated from HeLa^MR-1L cells. Similar amounts of HA-CRM were found in both organellar species after PK treatment. In contrast, OPA1, an IMM protein protruding towards the intermembrane space (13), was almost completely digested by PK in mitoplasts but not in mitochondria (Fig.4D). These results indicate that MR1-L protrudes from the IMM towards the mitochondrial matrix. Finally, the size of an *in vitro* translation product starting from position 33 was clearly higher than the size of the mature MR-1L protein (Fig.4E), indicating that the three PNKD mutations are all contained within the MTS.

Glyo II-specific activity (14) was significantly increased in both HeLa^MR-1L mitochondria and HeLa^MR-1M microsomes; however, the reaction was not saturable up to a D-lactoylglutathione concentration of 3.6 mM, the Km of the authentic Glyo II being 0.4 mM, suggesting that the activity associated with both MR-1 isoforms is spurious (Supplementary Material, Table S).
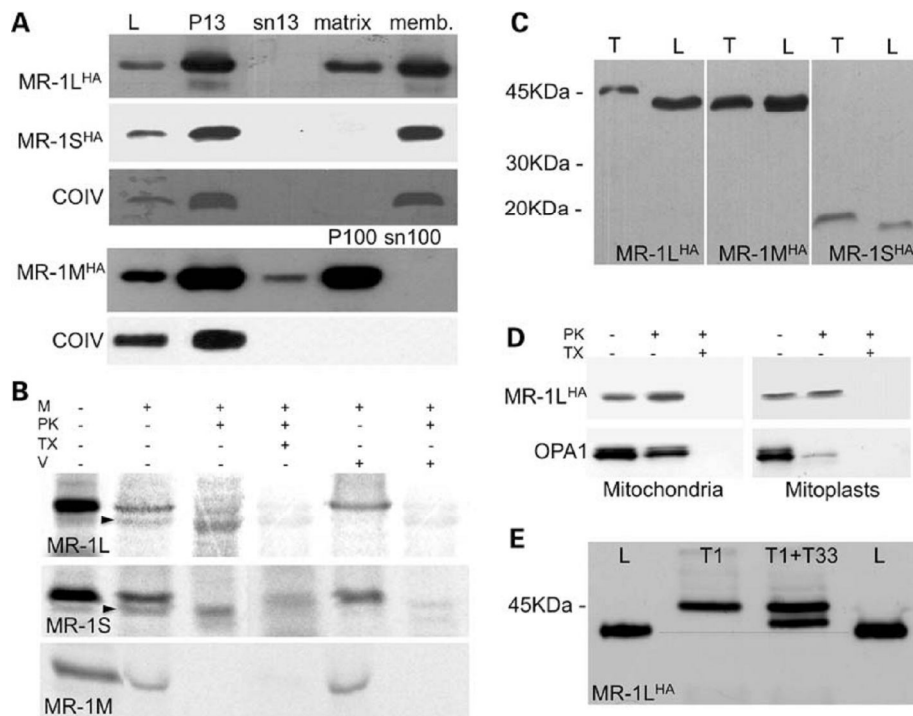
Figure4. WB analysis and *in vitro* import assay. (**A**) Subcellular localization of MR-1M^{HA}, MR-1L^{HA} and MR-1S^{HA} expressing HeLa cells. L, total lysate; P13, pellet of 13 000*g* fractions; sn13, 13 000*g* supernatant; P100, 100 000*g* pellet; sn100, 100 000*g* supernatant; memb., mitochondrial matrix and membranes. (**B**) *In vitro* import assay on isolated mouse liver mitochondria of the three MR-1 isoforms. M, mitochondria; PK, proteinase K; TX, Triton X100; V, valinomycin. Arrowheads show bands corresponding to mature protein species after MTS cleavage. (**C**) WB of SDS–polyacrylamide gel electrophoresis of *in vitro*-translated (T) versus recombinant HeLa cell lysates (L). Notice that MR-1L^{HA} and MR-1S^{HA} (mature) isoforms detected in cell lysates are smaller in size than the corresponding *in vitro*-translated species, which encompass the entire ORF of the cDNA. The T and L MR-1M^{HA} species are identical in size. (**D**) PK treatment of mitochondria and mitoplasts from MR-1L^{HA}-expressing HeLa cells. Anti-HA and anti-OPA1 antibodies were used. Lane 1: mitochondria; lane 2: mitochondria + PK; lane 3: mitochondria + PK + Triton X100; lane 4: mitoplasts; lane 5: mitoplasts + PK; lane 6: mitoplasts + PK + Triton X100. (**E**) WB analysis of recombinant MR-1L^{HA} variants. As shown by the dotted line, the mature MR-1L^{HA} protein species derived from recombinant HeLa cells (L) is smaller than the *in vitro*-translated protein species corresponding to the full-length precursor starting from the first methionine (T1), as well as the *in vitro* translation products starting from the positions corresponding to the PNKD mutation at position +33 (T33). These data demonstrate that the three known PNKD mutations, at position +7, +9 and +33, are all contained within the cleaved MTS.

Likewise, no obvious difference in the import process and in the amount of mature MR1-L protein was observed in HeLa^{MR-1L} cells carrying either mutation (Fig.5A–D). Both wild-type (wt) and mutant MR-1L^{HA} shared the same subcellular distribution, as demonstrated by both IF (Fig.5E) and WB analyses. Similar results were obtained with mutant variants of MR1-S^{HA}.
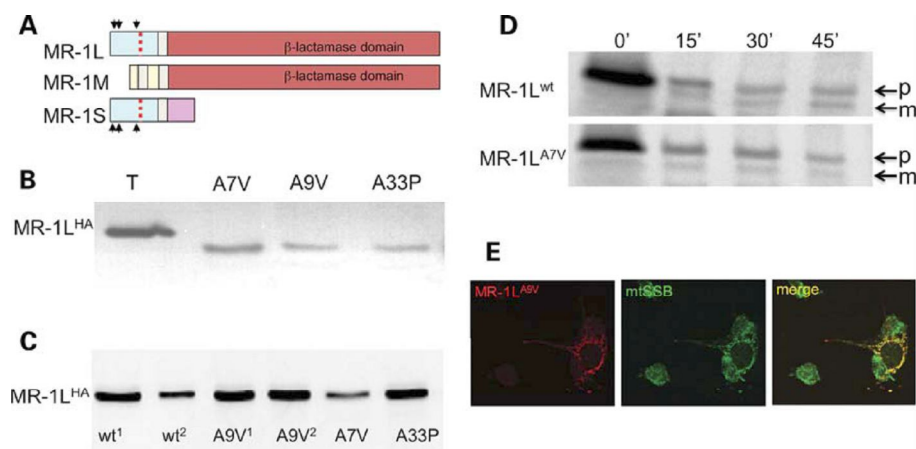
Figure5. Analysis of mutant MR-1L^{HA} protein species. (**A**) Scheme of MR-1 isoforms. (**B**) The mutant species are smaller than the *in vitro*-translated precursor protein (T), indicating that they are all converted into mature MR-1L^{HA} proteins. (**C**) WB analysis of MR-1L^{HA} wt and mutant variants in different recombinant HeLa cell lines. The amount of CRM varies randomly with no consistent difference between wt and mutant species. (**D**) Time course of *in vitro* import. No obvious difference is observed between mutant and wt. (**E**) The IF pattern in transiently expressing COS7 cells shows a mitochondrial localization of the A9V mutant MR-1L^{HA} variant.

DISCUSSION

Our results differ from those reported by Lee *et al*. (2), who attributed MR-1M to mitochondria, and MR1-S and MR-1L to the cytosol and plasma membrane. Irrespective of the reason for this discrepancy, for which we do not have an obvious explanation, our conclusions are based on several independent and unequivocal results, including (i) IF localization of recombinant proteins tagged with a short oligopeptide

at the C-terminus, (ii) WB analysis on subcellular and suborganellar fractions, (iii) protection from PK digestion and (iv) *in vitro* import assays. The latter showed that the size of the MTS common to MR1-S and MR1-L is compatible with the *in silico* prediction (39 amino acids), and is cleaved off during translocation, before the mature protein species are inserted in the IMM. The three mutations associated with PNKD are all contained within the MTS peptide and are therefore excluded from the mature protein species.

No obvious impairment in mitochondrial import and maturation processes was observed in MR-1 protein variants carrying either PNKD mutation. Although a more subtle alteration in the translocation kinetics cannot be excluded, this observation suggests that a novel mechanism of disease is at work in PNKD, involving directly the MTS rather than the mature, physiological form of the corresponding protein, which is normal in PNKD. One possibility is that the mutant precursor protein isoforms are toxic, although this is unlikely since the mutant species were correctly localized into mitochondria and processed to mature forms, as much as the wt ones. A more likely possibility is that the cleaved mutant MTS peptides can be directly deleterious to the host cells. For instance, the mutations could (i) reduce the degradability of the peptide causing its accumulation to toxic levels, or (ii) confer toxic properties, and/or (iii) promote its re-export and targeting to other compartments of the cell where, again, it could exert a damaging effect. Along this line, MTS peptides have been shown to alter the structural and functional integrity of mitochondrial membranes *in vitro* (15). A further consideration is that PNKD is a disease of the central nervous system

(CNS), and MR1-L expression is restricted to the brain (2,3). We confirmed this result by multi-tissue northern blot analysis (not shown). It is well possible that the processing of MR1-L in CNS cells, notably neurons, may be different from what we observed in cell cultures, and that the mutant MTS species can determine specific damage in nerve cells, more than in other cells, including alterations in their excitability and firing patterns. In any case, a toxic mechanism based on a gain of function of the mutant versus wt MTS is fully compatible with the dominant transmission of PNKD. *In silico* analysis (16) of the wt MR-1 MTS indicates the presence of two well-structured α-helices. Both the A7V and A9V changes are predicted to disrupt the second α-helix (Fig.1B), whereas the A33P could alter the C-terminal orientation of the MTS (Fig.1C). Further work is warranted to test experimentally whether and to what extent these structural changes can induce the mutant MR-1 MTS to act deleteriously within mitochondria or other parts of the cell.

MATERIALS AND METHODS

Cloning of MR-1 cDNA

Clones containing full ORFs of the three isoforms of MR-1, i.e. clone IOH6351 for MR-1L, clone IOH22386 for MR-1M and IRAUp969F0980D for MR-1S, were purchased from the RZPD Consortium (www.imagenes-bio.de). Three MR-1 full-length transcripts were 3'-tagged with the sequence encoding an epitope of the HA of the influenza virus.

Primers (Fw, forward; Rc, reverse complementary):

MR1S/L Fw:

gcgcggtgaagcggggggtgggccgccaccatggcggcggtggtagctgctacgg;

MR1S-HA Rc:

cggtttattcggtcaagcgtaatctggaacatcgtatgggtaggtctgcacccccagacccaac;

MR1M Fw:

ccgcccggccggcgcgtgcctgccgccaccatggcttggcagggctggcccg;

MR1M/L-HA Rc:

cggtttattcggtcaagcgtaatctggaacatcgtatgggtacttgctcttgtgcatatccttcag.

The constructs were inserted into the eukaryotic expression plasmid vector pcDNA3.1 (Invitrogen) by using suitable restriction sites.

Cell culture and transfection of HeLa and COS7 cells

Human cervix tumor (HeLa) and monkey kidney (COS7) cells were grown in Dulbecco's modified Eagle's medium supplemented with 10% fetal calf serum, 100 mg/ml streptomycin, 100 units/ml penicillin and 1 mM sodium pyruvate at 37°C in a humidified incubator containing 5% CO_2. The recombinant plasmids were transfected by electroporation in COS7 (for transient expression) or in HeLa (for stable expression) cells. Stably transfected clones of HeLa cells were selected under 800 ng/ml Geneticin (G418; Gibco-Invitrogen.).

Antibodies

The following antibodies were used in this work: mouse monoclonal and polyclonal anti-HA (Roche), anti-GM130 (Sigma), anti-clathrin (Cymbus Biotechnology), anti-PMP70 (Sigma), anti-SERCA2 ATPase (Sigma), anti-mitochondrial single-strand binding protein (anti-mtSSB) for IF studies; rat anti-HA (Roche), anti-OPA1, anti-CO I (Invitrogen), anti-CO IV (Invitrogen) for WB studies.

IF studies

Twenty-four to 48 h after electroporation, cells were plated on coverslips, fixed with 4% paraformaldehyde in PBS and lysed with PBS, 0.5% Triton X100. After blocking with NGS 15%, cells were incubated with primary antibodies in PBS, NGS 15%. Cells were washed with PBS three times each and incubated with fluorescent-dye-conjugated secondary antibodies (AlexaFluor, Molecular Probes), washed and analyzed with a Bio-Rad confocal microscope.

Mitochondrial import assay

Mitochondria from HeLa cells, freshly isolated as described elsewhere, were used to assaying protein import (17). ^{35}S radiolabeled *in vitro*-translated products corresponding to full-length ORFs were obtained with TNT Quick Coupled Transcription/Translation Systems (Promega). After incubation with freshly isolated mitochondria at 37°C in the presence or absence of 20 µM valinomycin, samples were washed and electrophoresed through a 12–14% SDS–polyacrylamide gel. After fixation in 10% acetic acid and 25% isopropanol, the gel was washed for 20 min in Amplify reagent (Amersham) and layered onto a phosphorimaging screen (Bio-Rad). After overnight exposure, autoradiography was carried out in a Molecular Imager apparatus (Bio-Rad).

PK protection

For PK protection, mitochondria and mitoplasts (12) from stably transfected MR-1L HeLa cells were incubated for 20 min at 37°C with 250 µg/ml PK or with 0.5% Triton X100, supplemented with 250 µg/ml PK.

Western blot

Approximately 2 x 10^6 cells were trypsinized, pelleted, sonicated and solubilized, as described elsewhere (18). SDS–polyacrylamide gel of 20–50 µg protein/lane and WB analysis were performed, and the HA-tagged proteins were immunovisualized by WB by the use of anti-HA antibody.

Cell fractionation

Standard methods were used for the preparation of mitochondrial enriched/postmitochondrial fractions in transfected cultured cells (8).

For suborganellar localization of MR-1S and MR-1L, mitochondria from transfected HeLa cells were resuspended in PK buffer and treated with three sonication strokes, and the membrane and soluble fractions were separated by ultracentrifugation at 100 000g for 1 h at 4°C. Mitoplasts were isolated from HeLa cells mitochondria by either digitonin treatment (19) or hypoosmotic shock (20). For subcellular localization of MR-1M, microsomal fraction was obtained from postmitochondrial supernatant of transfected HeLa cells after centrifugation at 100 000g for 1 h at 4°C. In some experiments, mitochondrial membranes from MR-1S and MR1-L transfected cells and microsomal fractions from MR-1M transfected cells were treated with non-ionic detergent deoxycholate (21) or with 0.1 M Na$_2$CO$_3$, pH 11.0 (17).

Site-directed mutagenesis

Modified cDNAs with point mutations leading to Ala7Val and Ala9Val changes were obtained on the basis of the wt HA-tagged

constructs by using QuikChange Site-Directed Mutagenesis Kit (Stratagene), using suitable primers (available upon request).

Biocomputational analysis

Prediction software for mitocondrial targeting or subcellular localization:

Mitoprot (ihg2.helmholtz-muenchen.de/ihg/mitoprot.html);

TargetP (www.cbs.dtu.dk/services/TargetP);

Predotar (urgi.versailles.inra.fr/predotar/predotar.html);

WoLF-PSORT (wolfpsort.org/).

Prediction software for trans-membrane domains:

TMPRED (www.ch.embnet.org/software/TMPRED_form.html);

TMHMM (www.cbs.dtu.dk/services/TMHMM/).

Multiple sequence alignments and phylograms were generated with Clustal W (22) and T-Coffee (23). Secondary structure was predicted with JPRED (24) and PSI-PRED (25).

Biochemical assays

Glyoxalase II (Glyo-II)-specific activity was measured spectrophotometrically after the glutathione-dependent reduction of DTNB [5,5'-di-thio-*bis*-(2)-nitrobenzoate] to TNB (thio-nitrobenzoate) at 412 nm by the use of *S*-lactoyl-glutathione (Sigma) as a substrate. The reaction was carried out at 37°C in 100 mM MOPS (3-[*N*-morpholino]-propanesulphonic acid), pH 7.5, 200 μM DTNB, 0.1% Triton X100 and 900 μM *S*-lactoyl-glutathione, with a molar extinction coefficient of 13.6 mM^{-1}.

SUPPLEMENTARY MATERIAL

Supplemental Table I. Biochemical Glyo II specific activity (in nmol min-1 mg-1)

HeLa[MR-1L] mitochondria	HeLa[Naïve] mitochondria	Ratio	Student's t-test p-value
10.7	3.85	2.8	0.0004
HeLa[MR-1M] microsomes	HeLa[Naïve] microsomes	Ratio	Student's t-test p-value
5.2	3.3	1.6	0.0002

Supplemental Table II. Transmembrane domain prediction.

	N°	Aminoacid range (TMpred)	Score (TMpred*)	Aminoacid range (TMHMM)	Score (TMHMM)
MR-1L	1	74-92	562	74-93	38%
MR-1M	2	11-29	2928	10-29	99%
		221-238	505	50-69	95%
MR-1S	1	74-91	2194	75-92	99%

* Significant values range from 500 (min.) to 3000 (max.)

Supplemental Figure 1
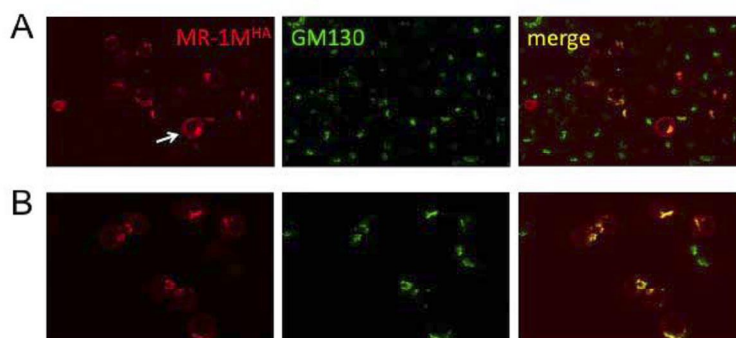
Subcellular localization of MR-1MHA in Hela cells In both fields most of the HA-specific CRM co-localizes with a marker for the Golgi apparatus. An arrow shows a cell with a pattern compatible with localization in the ER and plasma membrane.
Magnification 10x.

Conflict of Interest statement. None declared.

REFERENCES

1. Li T.B., Liu X.H., Feng S., Hu Y., Yang W.X., Han Y., Wang Y.G., Gong L.M. Characterization of MR-1, a novel myofibrillogenesis regulator in human muscle. Acta. Biochim. Biophys. Sin. (2004) 36:412–418.

2. Lee H.Y., Xu Y., Huang Y., Ahn A.H., Auburger G.W., Pandolfo M., Kwiecinski H., Grimes D.A., Lang A.E., Nielsen J.E., et al. The gene for paroxysmal non-kinesigenic dyskinesia encodes an enzyme in a stress response pathway. Hum. Mol. Gen. (2004) 13:3161–3170.

3. Rainier S., Thomas D., Tokarz D., Ming L., Bui M., Plein E., Zhao X., Lemons R., Albin R., Delaney C., et al. Myofibrillogenesis regulator 1 gene mutations cause paroxysmal dystonic choreoatethosis. Arch. Neurol. (2004) 61:1025–1029.

4. Chen D.H., Matsushita M., Rainier S., Meaney B., Tisch L., Feleke A., Wolff J., Lipe H., Fink J., Bird T.D., Raskind W.H. Presence of alanine-to-valine substitutions in myofibrillogenesis regulator 1 in paroxysmal nonkinesigenic dyskinesia: confirmation in 2 kindreds. Arch. Neurol. (2005) 62:597–600.

5. Stefanova E., Djarmati A., Momcilovic D., Dragasevic N., Svetel M., Klein C., Kostić V.S. Clinical characteristic of paroxysmal nonkinesigenic dyskinesia in Serbian family with myofibrillogenesis regulator 1 gene mutation. Mov. Disord. (2006) 21:2010–2015.

6. Hempelmann A., Kumar S., Muralitharan S., Sander T. Myofibrillogenesis regulator 1 gene (MR-1) mutation in an Omani family with paroxysmal nonkinesigenic dyskinesia. Neurosci. Lett. (2006) 402:118–120.

7. Tiranti V., Hoertnagel K., Carrozzo R., Galimberti C., Munaro M., Granatiero M., Zelante L., Gasparini P., Marzella R., Rocchi M., et al. Mutations of SURF-1 in Leigh disease associated with cytochrome c oxidase deficiency. Am. J. Hum. Genet. (1998) 63:1609–1621.

8. Fernandez-Vizarra E., Lopez-Perez M.J., Enriquez J.A. Isolation of biogenetically competent mitochondria from mammalian tissues and cultured cells. Methods (2002) 26:292–297.

9. Neupert W. Protein import into mitochondria. Annu. Rev. Biochem. (1997) 66:863–971.

10. Wiedemann N., Frazier A.E., Pfanner N. The protein import machinery of mitochondria. J. Biol. Chem. (2004) 279:14473–14476.

11. Gakh O., Cavadini P., Isaya G. Mitochondrial processing peptidases. Biochim. Biophys. Acta (2002) 1592:63–77.

12. Spinazzola A., Viscomi C., Fernandez-Vizarra E., Carrara F., D'Adamo P., Calvo S., Marsano R.M., Donnini C., Weiher H., Strisciuglio P., et al. MPV17 encodes an inner mitochondrial membrane protein and is mutated in infantile hepatic mitochondrial DNA depletion. Nat. Genet. (2006) 38:570–575.

13. Griparic L., van der Wel N.N., Orozco I.J., Peters P.J., van der Bliek A.M. Loss of the intermembrane space protein Mgm1/OPA1 induces swelling and localized constrictions along the lengths of mitochondria. J. Biol. Chem. (2004) 279:18792–18798.

14. Irsch T., Krauth-Siegel R.L. Glyoxalase II of African trypanosomes is trypanothione-dependent. J. Biol. Chem. (2004) 279:22209–22217.

15. Nicolay K., Laterveer F.D., van Heerde W.L. Effects of amphipathic peptides, including presequences, on the functional integrity of rat liver mitochondrial membranes. J. Bioenerg. Biomembr. (1994) 26:327–334.

16. Zhang Y.I. Tasser server for protein 3D structure prediction. BMC Bioinformatics (2008) 9:40.

17. Petruzzella V., Tiranti V., Fernandez P., Ianna P., Carrozzo R., Zeviani M. Identification and characterization of human cDNAs specific to BCS1, PET112, SCO1, COX15 and COX11, five genes involved in the formation and function of the mitochondrial respiratory chain. Genomics (1998) 54:494–504.

18. Tiranti V., Galimberti C., Nijtamns L., Bovolenta S., Perini M.P., Zeviani M. Characterization of SURF-1 expression and Surf-1p function in normal and disease conditions. Hum. Mol. Genet. (1999) 8:2533–2540.

19. Gallet P.F., Zachowski A., Julien R., Fellmann P., Devaux P.F., Maftah A. Transbilayer movement and distribution of spin-

labelled phospholipids in the inner mitochondrial membrane. Biochim. Biophys. Acta (1999) 1418:61–70.

20. Ohba M., Schatz G. Disruption of the outer membrane restores protein import to trypsin-treated yeast mitochondria. EMBO J. 6:2117–2122.

21. Fujiki Y., Hubbard A.L., Fowler S., Lazarow P.B. Isolation of intracellular membranes by means of sodium carbonate treatment: application to endoplasmic reticulum. J. Cell. Biol. (1982) 93:97–102.

22. Thompson J.D., Higgins D.G., Gibson T.J. CLUSTAL W: improving the sensitivity of progressive multiple sequence alignment through sequence weighting, position-specific gap penalties and weight matrix choice. Nucleic Acids Res. (1994) 22:4673–4680.

23. Notredame C., Higgins D.G., Heringa J. T-Coffee: a novel method for fast and accurate multiple sequence alignment. J. Mol. Biol. (2000) 302:205–217.

24. Cole C., Barber J.D., Barton G.J. The JPRED 3 secondary structure prediction server. Nucleic Acids Res. (2008) 36:W197–W201.

25. Kaur H., Raghava G.P. Prediction of beta-turns in proteins from multiple alignment using neural network. Protein Sci. (2003) 12:627–634